

Perspectives on the dynamics in loop effective black hole interior

Mehdi Assanioussi,^{1,*} Andrea Dapor,^{2,†} and Klaus Liegener^{2,‡}

¹*II. Institute for Theoretical Physics, University of Hamburg,
Luruper Chaussee 149, 22761 Hamburg, Germany.*

²*Department of Physics and Astronomy, Louisiana State University, Baton Rouge, LA 70803, USA.*

In the loop quantum gravity context, there have been numerous proposals to quantize the reduced phase space of a black hole, and develop a classical effective description for its interior which eventually resolves the singularity. However little progress has been made towards understanding the relation between such quantum/effective minisuperspace models and what would be the spherically symmetric sector of loop quantum gravity. In particular, it is not clear whether one can extract the phenomenological predictions obtained in minisuperspace models, such as the singularity resolution and the spacetime continuation beyond the singularity, from a calculation in full loop quantum gravity. In this paper, we present an attempt in this direction in the context of Kantowski-Sachs spacetime, through the proposal of two new effective Hamiltonians for the reduced classical model. The first is derived using Thiemann classical identities for the regularized expressions, while the second is obtained as a first approximation of the expectation value of a Hamiltonian operator in loop quantum gravity in a semi-classical state peaked on the Kantowski-Sachs initial data. We then proceed with a detailed analysis of the dynamics they generate and compare them with the Hamiltonian derived in General Relativity and the common effective Hamiltonian proposed in earlier literature.

I. INTRODUCTION

It is said that General Relativity (GR) predicts its own inconsistency in the form of singularities: these are unavoidable features of several GR solutions, and are expected to be cured by a more complete and fundamental theory of gravity – perhaps a quantum theory. In the case of Loop Quantum Gravity (LQG) [1–3], the best results we have are based on models in Loop Quantum Cosmology (LQC) [4–6] – a LQG-inspired quantization of cosmological minisuperspaces – in which the big bang singularity is replaced by a “big bounce” bridging a contracting classical universe with an expanding one via a region of high (but finite) curvature in which gravity becomes effectively repulsive [7–9].

The LQC program has also been directed towards the study of black hole singularities, due to the fact that the interior of a spherically symmetric black hole can be described in terms of a Kantowski-Sachs cosmological model [10]. Several models have been proposed using Ashtekar variables for the black hole interior [11–24], and almost all of them find the same qualitative conclusion: the singularity is resolved, being replaced by a space-like transition hypersurface, to the past of which there is a trapped region (the black hole region) and to the future of which there is an anti-trapped region (the white hole region). In other words, the singularity is replaced by a black hole to “white hole” transition.

Inspired from the results in standard LQC for a homogeneous and isotropic spacetime, the models from [17–24], although differing in the details such as the choices of regularisation parameters ϵ , all postulate an effective dynamics for the classical symmetry reduced system, obtained via replacing the reduced Ashtekar-Barbero connection in GR Hamiltonian by a regularized expression $a \rightarrow \sin(\epsilon a)/\epsilon$. However, there was another proposal to construct a quantum Hamiltonian for the LQC homogeneous and isotropic model which relies on the construction of the Hamiltonian operator in LQG [25–29]. Though considered

* mehdi.assanioussi@desy.de

† adapor1@lsu.edu

‡ liegener1@lsu.edu

in the early days of LQC [30–33], then proposed in the context of spherically symmetric quantum model [15], and later on in the context of effective LQC models [34], the idea of mimicking the construction of the Hamiltonian operator in LQG for LQC models was put aside. This was due to the impression that it does not lead to any significant difference with respect to the symmetry reduction method applied in standard LQC models. Yet, this impression turned out to not be entirely correct. Indeed, recent works [35, 36] have shown that the quantum and effective Hamiltonians in the LQC homogeneous and isotropic model present a relative agreement with the standard ones in the regime of GR, but they also display significant differences, in particular for the pre-bounce branch of the universe. The question therefore arises: what is the situation in the black hole context and what are the differences which arise, if at all, with respect to the standard treatment in LQC effective black hole models? The current work is dedicated to analyzing this question. In particular, we shall consider four Hamiltonians, and compare the phase space dynamics they generate for the black hole interior (taking initial conditions at the black hole horizon): i) GR reduced Hamiltonian, H_{cl} , which gives rise to the singular Schwarzschild solution; ii) the Hamiltonian studied in [21], $H_{\text{eff}}^{(1)}$, obtained via the aforementioned replacement in the GR reduced Hamiltonian; iii) a new proposal $H_{\text{eff}}^{(2)}$ obtained using Thiemann identities; iv) and the Hamiltonian $H_{\text{eff}}^{(3)}$ obtained from the expectation value of a LQG Hamiltonian [25, 26] in a coherent state peaked on Kantowski-Sacks initial data.

Before we proceed, some observations are in order: first, while in cosmology proposals (iii) and (iv) coincide [35, 36], there is no guarantee that this remains true in general (and, in fact, we shall see that it is not the case for a black hole). Hence, we treat them as two separate proposals here. Second, in all our investigations, we shall adopt the so-called μ_o -scheme for the choice of regulators. While this is known to lead to quantum geometry effects at low curvature in all models considered so far, it remains the simplest testing ground for conceptual ideas. Our purpose is to identify common qualitative features (such as singularity resolution and black hole to "white hole" transition) that are expected to survive after a more "physical" $\bar{\mu}$ -scheme is adopted. We also point out that the only known choice within the full theory of LQG is that of μ_o -scheme.

The structure of the paper is the following. In Section II, we start by briefly reviewing the Hamiltonian formulation of Kantowski-Sachs metrics in terms of Ashtekar-Barbero variables, identifying the canonical variables of this system and obtaining the form of the classical Hamiltonian H_{cl} . This Hamiltonian is then regularized following the approach of standard LQC models, thereby obtaining the form of $H_{\text{eff}}^{(1)}$. We finally follow the alternative construction based on [35–37] to find the new proposal $H_{\text{eff}}^{(2)}$, which takes into account Thiemann identities at the minisuperspace level [25, 26]. Section III is dedicated to the derivation of $H_{\text{eff}}^{(3)}$, that is, the effective Hamiltonian obtained from full LQG. First, we present the choice of graph, whose parameters are the inverse of the number of nodes in each of the three spatial directions, $\mu_{|i|}$ (with $i = 1, 2, 3$). Then, we observe that the leading order in the semiclassical expansion of the expectation value of the LQG Hamiltonian coincides with the GR Hamiltonian as regularized on the graph, H_{eff}^μ . Subsequently, we identify the fundamental variables (i.e., holonomies and fluxes) that describe the discrete Kantowski-Sachs geometry, and evaluate H_{eff}^μ in this case. Finally, we discuss that the qualitative behavior of the solutions of dynamics is captured by the first few orders of the expansion in the discreteness parameters $\mu_{|i|}$, which leads to the explicit expression of $H_{\text{eff}}^{(3)}$. In Section IV we solve numerically the dynamics of the four Hamiltonians under consideration, starting with initial conditions at the black hole horizon. We numerically solve the dynamics in all the cases and make a detailed comparison of the induced evolutions, finding that all the effective Hamiltonians produce a black hole to "white hole" transition. We also evaluate the mass associated to the "white hole" horizon as a function of the initial black hole mass and compare the different cases. Section V concludes the paper with a discussion of the results.

II. EFFECTIVE KANTOWSKI-SACHS A LA LQC

The interior of a spherically symmetric black hole is characterized by the fact that Schwarzschild radial coordinate r becomes timelike. The topology of the spatial slices (i.e., the surfaces of constant r) in the interior is therefore $\mathbb{R} \times \mathbb{S}^2$, and the line element reads (in natural units, $G = 1 = c$)

$$ds^2 = - \left(\frac{2M_{\text{bh}}}{r} - 1 \right)^{-1} dr^2 + \left(\frac{2M_{\text{bh}}}{r} - 1 \right) dt^2 + r^2 d\Omega^2 \quad (1)$$

By changing coordinates $(r, t) \rightarrow (T, R)$, with $R = t/L_R$ and $T = T(r)$ (L_R is a constant with dimension of length), we can express the metric in the form

$$ds^2 = -N(T)^2 dT^2 + L_R^2 f(T)^2 dR^2 + L_S^2 g(T)^2 d\Omega^2 \quad (2)$$

where f , g and the coordinates are dimensionless (the latter ranging in $R \in [0, 1]$, $\theta \in [0, \pi]$ and $\varphi \in [0, 2\pi]$ respectively), N is the lapse function and L_S is a constant with dimension of length. Comparison with (1) reveals that

$$f(T)^2 = \frac{2M_{\text{bh}}}{r} - 1, \quad g(T)^2 = \frac{r^2}{L_S^2}, \quad N(T)^2 dT^2 = \left(\frac{2M_{\text{bh}}}{r} - 1 \right)^{-1} dr^2 \quad (3)$$

Let us consider (2) in its generality, that is, keeping f , g and N general functions of T . Then, we have what is called a Kantowski-Sachs model. This model can be described as a Hamiltonian system using the Ashtekar-Barbero formulation of GR [38–40]. In this formulation, the system is described via a phase space coordinatized by dynamical variables (a, b, p_a, p_b) and a Hamiltonian constraint $H_{\text{cl}}(a, b, p_a, p_b)$ generating their evolution with respect to T . The relation between the dynamical variables and the metric components are set as

$$|p_a| = L_S^2 g^2, \quad |p_b| = 2L_R L_S |fg| \quad (4)$$

while the conjugated variables a and b satisfy the Poisson algebra

$$\{a, p_a\} = \frac{\kappa\beta}{8\pi}, \quad \{b, p_b\} = \frac{\kappa\beta}{8\pi} \quad (5)$$

where $\kappa = 16\pi G/c^3$. The explicit form of Ashtekar-Barbero variables is

$$\begin{aligned} A_R^R &= -a, & A_\theta^\theta &= -b, & A_\varphi^\varphi &= -b \sin \theta, & A_\varphi^R &= -\cos \theta \\ E_R^R &= |p_a| \sin \theta, & E_\theta^\theta &= \frac{p_b}{2} \sin \theta, & E_\varphi^\varphi &= \frac{p_b}{2} \end{aligned} \quad (6)$$

where β is the Barbero-Immirzi parameter of LQG. It follows that the Hamiltonian reads

$$H_{\text{cl}} = -N \frac{8\pi}{\kappa\beta^2} \frac{\text{sgn}(p_b)}{\sqrt{|p_a|}} \left[2ab|p_a| + (b^2 + \beta^2) \frac{p_b}{2} \right] \quad (7)$$

The equations of motion generated by this H_{cl} can be solved analytically by for a clever choice of lapse function (namely, $N = \text{sgn}(p_b)\sqrt{|p_a|}$), and give

$$\begin{aligned} a(T) &= a^0 \cos \left(\frac{T - T_0}{2} \right)^{-4 \text{ sgn}(p_a^0)}, & p_a(T) &= p_a^0 \cos \left(\frac{T - T_0}{2} \right)^{4 \text{ sgn}(p_a^0)} \\ b(T) &= -\beta \tan \left(\frac{T - T_0}{2} \right), & p_b(T) &= \frac{2}{\beta} a^0 p_a^0 \sin(T - T_0) \end{aligned} \quad (8)$$

where $a(T_0) = a^0$ and $p_a(T_0) = p_a^0$ are integration constants, while $b(T_0) = 0 = p_b(T_0)$ identify $T = T_0$ with the black hole horizon. To give physical meaning to the integration constants, we plug (8) in the metric components of Kantowski-Sachs line element. Using the equations for p_a in (4) and (8), and imposing the second condition in (3), we identify $r = \sqrt{|p_a^0|} \cos[(T - T_0)/2]^2 \operatorname{sgn}(p_a^0)$. At this point, note that since r decreases as we go further inside the black hole, the sign of p_a^0 must be positive and therefore $\operatorname{sgn}(p_a^0) = +1$. It follows that

$$L_R^2 f^2 = \frac{p_b^2}{4|p_a|} = \frac{(a^0)^2 p_a^0}{\beta^2} 4 \sin\left(\frac{T - T_0}{2}\right)^2 \cos\left(\frac{T - T_0}{2}\right)^{-2} = 4 \frac{(a^0)^2 p_a^0}{\beta^2} \left(\frac{\sqrt{p_a^0}}{r} - 1\right) \quad (9)$$

The first condition in (3) then implies $\sqrt{p_a^0} = 2M_{\text{bh}}$ and $a^0 = \pm\beta L_R/(4M_{\text{bh}})$. In other words, if we want to obtain dynamically the line element in Schwarzschild coordinates (with the choice $R = t/L_R$), we must choose initial conditions at the black hole horizon¹ as

$$a(T_0) = a^0 := \pm \frac{\beta L_R}{4M_{\text{bh}}}, \quad b(T_0) = b^0 := 0, \quad p_a(T_0) = p_a^0 := 4M_{\text{bh}}^2, \quad p_b(T_0) = p_b^0 := 0 \quad (10)$$

In the following, we shall choose $a^0 > 0$ (and $L_R = 1$ in standard units), so as to ensure that the flow of H_{cl} is parametrized by an increasing T (i.e. $T \geq T_0$). Note also that the singularity is identified by the condition $p_a = 0$, occurring at the point $T = \pi + T_0$, and it translates into a diverging spatial curvature.

In the context of LQC, several quantizations of this model have been proposed [17–23]. It has been conjectured that the qualitative description of the semiclassical dynamics in these quantum models can be reproduced by classical effective models. These effective models are defined on the classical phase space with a dynamics generated by an effective Hamiltonian obtained by appropriately modifying the classical Hamiltonian (7). The common choice of effective Hamiltonian is obtained by the replacements

$$a \rightarrow \frac{\sin(\mu_a a)}{\mu_a}, \quad b \rightarrow \frac{\sin(\mu_b b)}{\mu_b} \quad (11)$$

where μ_a and μ_b are phase space functions determined by the quantum model. The effective Hamiltonian therefore reads

$$H_{\text{eff}}^{(1)} = -N \frac{8\pi}{\kappa\beta^2} \frac{\operatorname{sgn}(p_b)}{\sqrt{|p_a|}} \left[2 \frac{\sin(\mu_a a)}{\mu_a} \frac{\sin(\mu_b b)}{\mu_b} |p_a| + \left(\frac{\sin(\mu_b b)^2}{\mu_b^2} + \beta^2 \right) \frac{p_b}{2} \right] \quad (12)$$

It was shown in [21] that in the case where μ_a and μ_b are chosen to depend on the initial conditions², the solutions to the equations of motion with $H_{\text{eff}}^{(1)}$ display a resolution of the singularity and a transition from a black hole interior to a white hole like interior with a second horizon at an instant T_{wh} . We will display more details about this effective model in section IV.

An alternative effective Hamiltonian can be obtained following the approach which was advocated in [34, 37] in the context of LQC, and which relies on the regularization of the classical Hamiltonian used in the LQG approach. In the context of LQC [35, 36] the alternative regularization gave rise to a dynamics significantly different from the standard one. It is based on the classical relations referred to as Thiemann identities. In particular, one of them states that the extrinsic curvature can be expressed in terms of a Poisson bracket: $K_a^I = \{A_a^I, K(A, V)\}$, where $K(A, V)$ is a polynomial involving the connection A the spatial volume V and its Poisson-brackets. However, as soon as a phase space function involve Poisson-bracket, the "regularization" maps ι and "symplectic reduction" map ω do not commute. Explicitly,

¹ One can check that with these values the last condition in (3) is also satisfied.

² This choice is referred to as the *generalized μ_o -scheme* [24], as opposed to the standard μ_o -scheme where the μ parameters are fixed positive numbers (which we use in this article), and the $\bar{\mu}$ -scheme where the μ parameters are chosen to depend explicitly on the phase space variables.

considering the maps $\omega : (A, E) \mapsto (a, p_a, b, p_b)$ via (6) and $\iota_{A,E} : (A, E) \mapsto (h, E)$ via (17) and lastly $\iota_{a,b}$ as (11) then in general, for two polynomials f, g we have

$$\begin{aligned} \iota_{a,b}(\{\omega \circ f(A, E), \omega \circ g(A, E)\}) &\neq \{\iota_{a,b} \circ \omega \circ f(A, E), \iota_{a,b} \circ \omega \circ g(A, E)\} \\ &\neq \{\omega \circ \iota_{A,E} \circ f(A, E), \omega \circ \iota_{A,E} \circ g(A, E)\} \\ &\neq \omega(\{\iota_{A,E} \circ f(A, E), \iota_{A,E} \circ g(A, E)\}) \end{aligned} \quad (13)$$

$H_{\text{eff}}^{(1)}$ is obtained using the first sequence of mappings on the first line of (13) to compute K_a^I , while the new proposal $H_{\text{eff}}^{(2)}$ uses the second sequence of mappings³ on the first line and produces the following effective Hamiltonian

$$\begin{aligned} H_{\text{eff}}^{(2)} = N \frac{8\pi \text{sgn}(p_b)}{\kappa \sqrt{|p_a|}} &\left[2 \frac{\sin(\mu_a a)}{\mu_a} \frac{\sin(\mu_b b)}{\mu_b} |p_a| + \left(\frac{\sin(\mu_b b)^2}{\mu_b^2} - 1 \right) \frac{p_b}{2} \right. \\ &\left. - \frac{1 + \beta^2}{\beta^2} \frac{\sin(\mu_b b)}{\mu_b} (\cos(\mu_a a) + \cos(\mu_b b)) \left(|p_a| \frac{\sin(\mu_a a)}{\mu_a} \cos(\mu_b b) + \frac{p_b}{8} \frac{\sin(\mu_b b)}{\mu_b} (\cos(\mu_a a) + \cos(\mu_b b)) \right) \right] \end{aligned} \quad (14)$$

Note that both effective Hamiltonians (12) and (14) converge to H_{cl} in the limit $\mu_a, \mu_b \rightarrow 0$, ensuring the recovery of the continuum limit.

Another avenue in order to obtain a loop-effective model is to attempt to derive the effective Hamiltonian from the quantum theory. An approach following this point of view is to consider the expectation value of the Hamiltonian operator on a family of semiclassical states peaked on points of the classical phase space. This has been realized for instance in the case of homogeneous cosmology (within QRLG [41] and LQG [37, 42]). In fact, in homogeneous isotropic LQC such expectation value coincides with the effective Hamiltonian obtained by the rule (11), thereby motivating the replacement method [43]. In the case of spherically symmetric black holes, this expectation value approach has been applied in QRLG to derive an effective Hamiltonian. In the next section, we derive an effective Hamiltonian for Kantowski-Sachs using this method in LQG.

III. EFFECTIVE KANTOWSKI-SACHS FROM LQG

Our approach in the case of the interior region of a black hole is the same as the one adopted for flat homogeneous and isotropic cosmology [35, 37]. Namely, the starting point is to consider a semi-classical coherent state on the Hilbert space of loop quantum gravity \mathcal{H} , peaked on the classical configuration of interest (for more details on coherent states in LQG, see [44–53]). Then one computes the leading order, in a semi-classical expansion, of the expectation value of the LQG Hamiltonian operator originally proposed by Thiemann in its graph non-changing version [25, 26, 54, 55] on the chosen semi-classical state. The obtained leading order is what one considers as the Hamiltonian in the effective theory⁴.

The calculation of the expectation value of the LQG Hamiltonian operator on a semi-classical state is in general involved. However, the calculation of the leading order of the expectation value is easier thanks to the properties of the semi-classical state. Indeed, the computations reduce to the replacement in the Hamiltonian of holonomy and flux operators by their classical, discretised expressions $\iota_{A,E}(A), \iota_{A,E}(E)$. The commutators are replaced by Poisson brackets on the discretised phase-space. These are then computed via the third line in (13), where we perform the symplectic reduction with respect to the discretised geometry on which the semi-classical state is peaked.

³ In the case of isotropic LQC the four sequences of mappings in (13) agree.

⁴ For example, one could use the complexifier coherent states from [44–46]. This has been done in [48], however - in contrast with the discretization considered here - with a different choice of coordinates and discretized phase space functions, i.e. gauge covariant fluxes. For further implications on these different fluxes see [56, 57].

The first step is therefore to perform a discretization of the spacetime manifold using a choice of graph and its dual 2-complex. Since we are interested in a spacetime of the Kantowski-Sachs type, we choose the graph Γ to be adapted to the cylindrical coordinates in which the Kantowski-Sachs metric is expressed (2). Such choice of graph simplifies considerably the calculations. Thus, we are interested in a fixed graph Γ , which is chosen to be a compact subset of the cubic lattice \mathbb{Z}^3 embedded in $[0, 1] \times \mathbb{S}^2$. We choose a graph Γ which has a finite number of vertices equal to the product $N_1 N_2 N_3$ where $N_1, N_2, N_3 \in \mathbb{N}$ are the numbers of vertices in the directions R, θ and φ respectively. Finally, the cubic lattice Γ is oriented the following way: at each vertex v there are six edges $e_{v,i}$ ($i = \pm 1, \pm 2, \pm 3$ such that 1, 2, 3 correspond to the directions R, θ and φ respectively, while + is for outgoing edges and - for incoming edges) starting at v and going along the directions i (with constant coordinates along the remaining directions). The coordinate lengths of these edges are $\mu_1 L_R, \mu_2 L_S$ and $\mu_3 L_S$, where we define

$$\mu_1 = \frac{1}{N_1}, \quad \mu_2 = \frac{\pi}{N_2 + 1}, \quad \mu_3 = \frac{2\pi}{N_3} \quad (15)$$

Therefore, the coordinates $(R_v, \theta_v, \varphi_v) =: v$ of a generic vertex v in the graph take values in

$$R_v \in \left\{ \mu_1, 2\mu_1, \dots, 1 \right\}, \quad \theta_v \in \left\{ \mu_2, 2\mu_2, \dots, \pi - \mu_2 \right\}, \quad \varphi_v \in \left\{ \mu_3, 2\mu_3, \dots, 2\pi \right\}. \quad (16)$$

In the following, we present the discrete version of the Kantowski-Sachs system on the graph Γ and the corresponding holonomies and fluxes.

A. Discretization of Kantowski-Sachs

The discrete model of Kantowski-Sachs solution is obtained by introducing the holonomy-flux algebra as discrete objects associated with the edges of the graph Γ , given by the semi-classical state we chose and described above, and surfaces of the dual 2-complex. These surfaces are obtained in the following way: at each edge $e_{v,i}$ we consider the surface $S_{e_{v,i}}$ orthogonal to it at the midpoint and oriented in the direction i , such that it has sides of coordinate lengths $\mu_{|j|}$ and $\mu_{|k|}$ ($j, k \neq \pm i$) parallel to the edges of the graph Γ . Then, we define the holonomies h and the fluxes E_I as

$$h(e_{v,i}) := \mathcal{P} \exp \left(- \int_0^1 ds \dot{e}_{v,i}^a(s) A_a^I(e_{v,i}(s)) \tau_I \right), \quad E_I(e_{v,i}) := \int_{S_{e_{v,i}}} dx^a \wedge dx^b \epsilon_{abc} E_I^c(\vec{x}) \quad (17)$$

where $\dot{e}_{v,i}$ is the normalized tangent vector to the edge $e_{v,i}$ at v , and we choose the explicit basis $\tau_I = -i\sigma_I/2$ of $\mathfrak{su}(2)$, i.e. $[\tau_I, \tau_J] = \epsilon_{IJK} \tau_K$.

The leading order of the expectation value of Thiemann Hamiltonian operator, which we denote H_{eff}^μ , takes the form

$$H_{\text{eff}}^\mu := N(H_E^\mu + H_L^\mu) \quad (18)$$

where

$$H_E^\mu := \frac{-4}{\kappa^2 \beta} \sum_{v \in V(\Gamma)} \frac{1}{T_v} \sum_{i,j,k} \epsilon(e_{v,i}, e_{v,j}, e_{v,k}) \text{tr} \left((h(\square_{ij}^v) - h(\square_{ij}^v)^\dagger) h(e_{v,k})^\dagger \{h(e_{v,k}), V^\mu\} \right) \quad (19)$$

and

$$H_L^\mu := \frac{64(1 + \beta^2)}{\kappa^4 \beta^7} \sum_{v \in V(\Gamma)} \frac{1}{T_v} \sum_{i,j,k} \epsilon(e_{v,i}, e_{v,j}, e_{v,k}) \text{tr} \left(h(e_{v,i})^\dagger \{h(e_{v,i}), K\} h(e_{v,j})^\dagger \{h(e_{v,j}), K\} h(e_{v,k})^\dagger \{h(e_{v,k}), V^\mu\} \right) \quad (20)$$

with V^μ being the discrete volume given as

$$V^\mu := \sum_{v \in V(\Gamma)} \sqrt{\frac{1}{T_v} |Q_v|}, \quad Q_v = \sum_{i,j,k} \epsilon(e_{v,i}, e_{v,j}, e_{v,k}) \epsilon^{IJK} E_I(e_{v,i}) E_J(e_{v,j}) E_K(e_{v,k}) \quad (21)$$

and $K := \{V^\mu, H_E^\mu\}$. The factor $\epsilon(e_{v,i}, e_{v,j}, e_{v,k}) = \text{sgn}(\det(\dot{e}_{v,i}, \dot{e}_{v,j}, \dot{e}_{v,k}))$ and $V(\Gamma)$ is the set of all vertices of the graph. Note that the six-valent vertices have $T_v = 48$, while the five-valent vertices with $R_v = \mu_1, 1$ or $\theta_v = \mu_2, \pi - \mu_2$ have $T_v = 24$. The symbol $h(\square_{ij}^v)$ corresponds to the holonomy, along the oriented loop \square_{ij}^v , defined as

$$h(\square_{ij}^v) := h(e_{v+\mu_{|j|}\dot{e}_{v,j}, -j}) h(e_{v+\mu_{|i|}\dot{e}_{v,i}+\mu_{|j|}\dot{e}_{v,j}, -i}) h(e_{v+\mu_{|i|}\dot{e}_{v,i}, j}) h(e_{v,i}) \quad (22)$$

The final expressions for the quantities H_E^μ and H_L^μ in terms of the phase space variables $\{a, b, p_a, p_b\}$ are obtained by first performing the calculation of the Poisson brackets involved on the level of the general holonomy-flux algebra, then evaluating the holonomies and fluxes for the Kantowski-Sachs metric. These are

$$\begin{aligned} E_I(e_{v,\pm 1}) &= \pm \delta_{I1} 2|p_a| \sin(\theta_v) \sin(\frac{\mu_2}{2}) \mu_3, & h(e_{v,\pm 1}) &= \exp(\mp a \tau_1 \mu_1), \\ E_I(e_{v,\pm 2}) &= \pm \delta_{I2} \frac{p_b}{2} \sin(\theta_v \pm \frac{\mu_2}{2}) \mu_1 \mu_3, & h(e_{v,\pm 2}) &= \exp(\mp b \tau_2 \mu_2), \\ E_I(e_{v,\pm 3}) &= \pm \delta_{I3} \frac{p_b}{2} \mu_2 \mu_1, & h(e_{v,\pm 3}) &= \exp(\mp \mu_3 (b \sin(\theta_v) \tau_3 - \cos(\theta_v) \tau_1)) \end{aligned} \quad (23)$$

These computations produce an analytic expression for H_{eff}^μ which is too lengthy to fit in an article, due to the lengthy expression of H_L^μ . For the sake of the argument, we display the expression of H_E^μ :

$$\begin{aligned} H_E^\mu &= \text{sgn}(p_b) \frac{2\pi}{\kappa \sqrt{|p_a|}} \sum_{\theta=\mu_2}^{N_2 \mu_2} \mu_2 \left[\sqrt{\frac{\tan(\mu_2/2)}{\mu_2/2}} 2|p_a| \sin(\theta) \frac{\sin(a\mu_1)}{\mu_1} \right. \\ &\quad \times \left(b \frac{\sin(2\mu_3 \chi(\theta))}{2\mu_3 \chi(\theta)} + \cos(\frac{\mu_2}{2}) \frac{\sin(b\mu_2)}{\mu_2} \frac{b^2 \sin(\theta)^2 + \cos(\theta)^2 \cos(\mu_3 \chi(\theta))}{b^2 \sin(\theta)^2 + \cos(\theta)^2} \right) \\ &\quad + \sqrt{\frac{\mu_2}{2} \cot(\frac{\mu_2}{2})} \frac{p_b}{2} \left(\cos(\theta) \frac{\sin(\mu_3 \chi(\theta))}{\mu_3 \chi(\theta)} \frac{\cos(\mu_3 \chi(\theta - \mu_2)) - \cos(\mu_3 \chi(\theta + \mu_2))}{\mu_2} \right. \\ &\quad \left. \left. + \cos(\mu_3 \chi(\theta)) \frac{1}{\mu_2} \sum_{s=\pm 1} s \frac{\sin(\mu_3 \chi(\theta + s\mu_2))}{\mu_3 \chi(\theta + s\mu_2)} (\cos(\theta + s\mu_2) \cos(b\mu_2) + b \sin(\theta + s\mu_2) \sin(b\mu_2)) \right) \right] \end{aligned} \quad (24)$$

where $\chi(\theta) := \frac{1}{2} \sqrt{b^2 \sin(\theta)^2 + \cos(\theta)^2}$. Unfortunately, the complexity of the expression of H_{eff}^μ makes it at the moment impossible to solve the equations of motion neither analytically nor numerically. However, since conceptually we are interested in large graphs, the values of the parameters $\mu_{|i|}$ are considered to be very small compared to unity (see (15)). Hence, we take the power series expansion of H_{eff}^μ in $\mu_{|i|}$. In

particular, we evaluate the expansion up to second order in $\mu_{|i|}$, giving the following expression

$$\begin{aligned} H_{\text{eff}}^{(3)} := & -N \frac{8\pi \operatorname{sgn}(p_b)}{\kappa \beta^2 \sqrt{|p_a|}} \left[2ab|p_a| + (b^2 + \beta^2) \frac{p_b}{2} \right] \\ & + N \frac{\pi \operatorname{sgn}(p_b)}{144\kappa \beta^2 \sqrt{|p_a|}} \left[96\mu_1^2 a^2 b \left(2a(3\beta^2 + 5)|p_a| + 3b(\beta^2 + 1)p_b \right) \right. \\ & + 24\mu_2^2 \left(2ab|p_a| (18b^2\beta^2 + 2(11b^2 + 6\beta^2) + 17) + p_b (2(3\beta^2 + 5)b^4 + 3b^2 + 7\beta^2) \right) \\ & \left. + \mu_3^2 \left(2ab|p_a| (288b^2\beta^2 + (352b^2 + 3\beta^2) + 59) + b^2 p_b (96b^2\beta^2 + 5(32b^2 + 9\beta^2) - 19) \right) \right] \end{aligned} \quad (25)$$

IV. COMPARATIVE ANALYSIS OF THE EFFECTIVE DYNAMICS

In this section we expose the analysis of the dynamics in the effective Kantowski-Sachs models described by the three Hamiltonians $H_{\text{eff}}^{(1)}$, $H_{\text{eff}}^{(2)}$ and $H_{\text{eff}}^{(3)}$ presented in the previous sections. Specifically, we compare the solutions to the equations of motion induced by the aforementioned Hamiltonians and we discuss the qualitative aspects featuring in each case: in particular, the resolution of the singularity and the “white hole”-like region.

The equations of motion that we are solving for the variables a , b , p_a and p_b are of the form

$$\dot{a}(T) = \{a(T), H_{\text{eff}}^{(i)}\}, \quad \dot{b}(T) = \{b(T), H_{\text{eff}}^{(i)}\}, \quad \dot{p}_a(T) = \{p_a(T), H_{\text{eff}}^{(i)}\}, \quad \dot{p}_b(T) = \{p_b(T), H_{\text{eff}}^{(i)}\}, \quad (26)$$

where i ranges from 1 to 3. With a suitable choice of lapse function, these equations can be solved analytically in the case of the Hamiltonian $H_{\text{eff}}^{(1)}$ [17, 21], but this is so far not the case for the other two Hamiltonians. However one can proceed with solving the equations of motion numerically with a lapse function fixed as earlier $N = \operatorname{sgn}(p_b)\sqrt{|p_a|}$ and for the initial conditions (10), then compare the solutions for the various dynamics considered. As already discussed, the initial conditions (10) are set to reproduce Schwarzschild line element in the chosen coordinates, allowing us to interpret the resulting dynamics as the (effective) evolution of the interior of a Schwarzschild black hole. It is important to point out that the value of a^0 is in principle free (if we chose $a^0 = \lambda\beta L_R/(4M_{\text{bh}})$, then it simply means that $R = \lambda^{-1}t/L_R$), we will discuss this particular point about the relevance of the choice of a^0 in the effective models later in this section. As we discuss later, we observe that for the three effective Hamiltonians we consider, the singularity is avoided.

The other important element of our analysis is the choice of μ_a and μ_b . While it might be argued that a $\bar{\mu}$ -scheme (in which these regulators are phase space functions) is more physical, there is currently no agreement on the correct choice. Moreover, as pointed out in [24], the choice of μ 's as dependent on the initial conditions (that is the generalized μ_0 -scheme, for example $\mu_b = \sqrt{\Delta/p_a^0}$ adopted in [21]), implicitly assumes that μ 's are constants of motion; however, the fact that the regulator is a phase space function (albeit conserved by the dynamics) implies that the equations of motion for the fundamental variables (a, b, p_a, p_b) are different from those computed in the μ_0 -scheme (i.e., with μ 's constant on the whole phase space). While it might be possible to circumvent these issues by relying on an extended phase space (where the regulator become themselves new phase space coordinates), we prefer to refrain from introducing these complications, and thus stick to the original μ_0 -scheme. From the point of view of the full theory, this is so far the only choice, since in $H_{\text{eff}}^{(3)}$ the regulators μ_1 , μ_2 and μ_3 are given in terms of the numbers of nodes (15). For our analysis, we use the identification

$$\mu_1 = \mu_a = \mu_a^0, \quad \mu_2 = \mu_3 = \mu_b = \mu_b^0, \quad (27)$$

where μ_a^o and μ_b^o are fixed positive numbers. Now we can proceed with the analysis of the effective evolution. In figure 1 we display the evolution trajectories of p_b as a function of $\log(p_a)$, obtained for an initial mass $M_{\text{bh}} = 10$ in Planck units. The plots in figure 1 show that all the effective solutions display

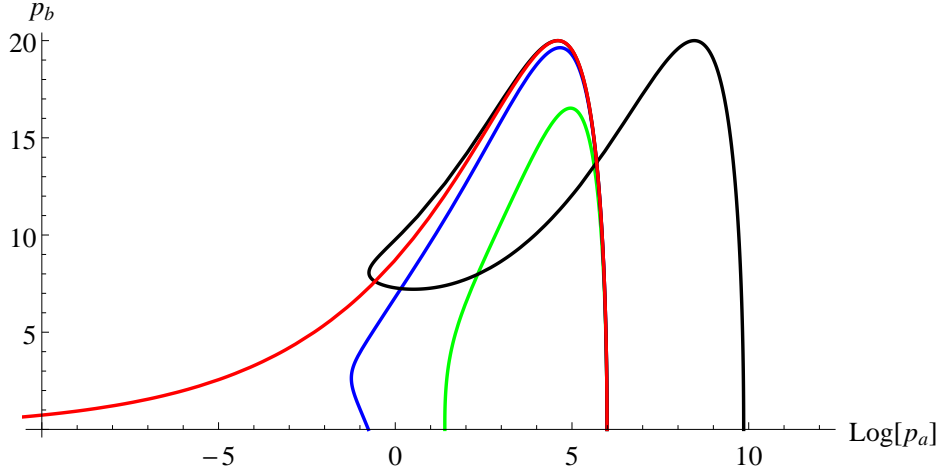


Figure 1. The evolution of $p_a(T)$ and $p_b(T)$ with the initial conditions (10) for $M_{\text{bh}} = 10$ in Planck units. The red, black, blue and green trajectories correspond respectively to the solutions obtained using the Hamiltonians H_{cl} , $H_{\text{eff}}^{(1)}$, $H_{\text{eff}}^{(2)}$ and $H_{\text{eff}}^{(3)}$. We take $G = c = 1$, $\beta = 0.2375$, $\mu_a = 1/5$ and $\mu_b = \pi/4$.

a non-vanishing minimum for p_a , implying an absence of the singularity predicted by classical GR and the presence of a bounce at specific times which we denote $T_b^{(i)}$. We also observe that all the effective trajectories for p_b reach a vanishing value at some negative times $T_{\text{wh}}^{(i)}$, indicating the presence of a Killing horizon in the effective solutions. Through the evaluation of the geodesics expansions⁵ $\Theta_{\pm} = \dot{p}_a/(\sqrt{2}p_a N)$ associated to the two future-oriented null normals to the surfaces of T and R constant, we observe that Θ_{\pm} have the same signs throughout the evolution and correspond to the sign of \dot{p}_a/N (since p_a remains positive throughout the evolution), which is independent of the choice of the coordinates. Namely, it is negative in the region $0 < T < T_b$ and positive in the region $T_b < T < T_{\text{wh}}$, while vanishing at T_b . Therefore the boundary $T = T_b$ is a transition surface from a trapped region – the black hole interior – to an anti-trapped region – the “white hole”-like interior.

The presence of a bounce and a second horizon were already observed in the analysis of the dynamics generated by $H_{\text{eff}}^{(1)}$ in [21] – although we recall that here we are using a different choice of regulators. While the bounce seems to be a generic feature, the presence of a second Killing horizon is more subtle. For example, in the context of QRLG [58, 59] and within a specific $\bar{\mu}$ -scheme, no second horizon was present in the solutions to the effective dynamics. In presence of a second horizon, an interesting feature to analyze is the mass M_{wh} associated to such horizon, and investigate its possible dependence on the initial mass of the black hole M_{bh} . The white hole mass is given by

$$M_{\text{wh}}^{(i)} := \frac{\sqrt{p_a^{(i)}(T_{\text{wh}}^{(i)})}}{2} \quad (28)$$

where $T_{\text{wh}}^{(i)}$ is the value of $T \neq T_0$ at which $p_b^{(i)}$ vanishes. Note that in general, $M_{\text{wh}}^{(i)}$ depends on the initial condition a^0 , which classically is an irrelevant quantity (due to the fact that, under coordinate

⁵ Expansion parameters are defined as $\Theta_{\pm} = h^{\alpha\beta}\nabla_{\alpha}k_{\beta}^{\pm}$ where $h_{\alpha\beta}$ is the metric induced by $g_{\mu\nu}$ on the 2-spheres coordinatized by (θ, φ) and k^{\pm} are the vector fields tangent to the congruences of outgoing and ingoing radial null geodesics – given here by $k_a^+ = 1/\sqrt{2}(-N, L_R f, 0, 0)$ and $k_a^- = 1/\sqrt{2}(-N, -L_R f, 0, 0)$ respectively.

transformation $R \rightarrow \lambda R$, the variable a scales as $a \rightarrow \lambda^{-1}a$). Following the perspective of an observer whose coordinate system is given in (2) and produces the classical Schwarzschild line element, a^0 is fixed as in (10).

From the analysis of the evolution with different initial masses, the relations between black hole mass and the mass associated to the “white hole” horizon, induced by the different Hamiltonians we considered, have the same asymptotic dependence on M_{bh} , namely $M_{\text{wh}} \propto M_{\text{bh}}$ (see figure 2). At this point, it is

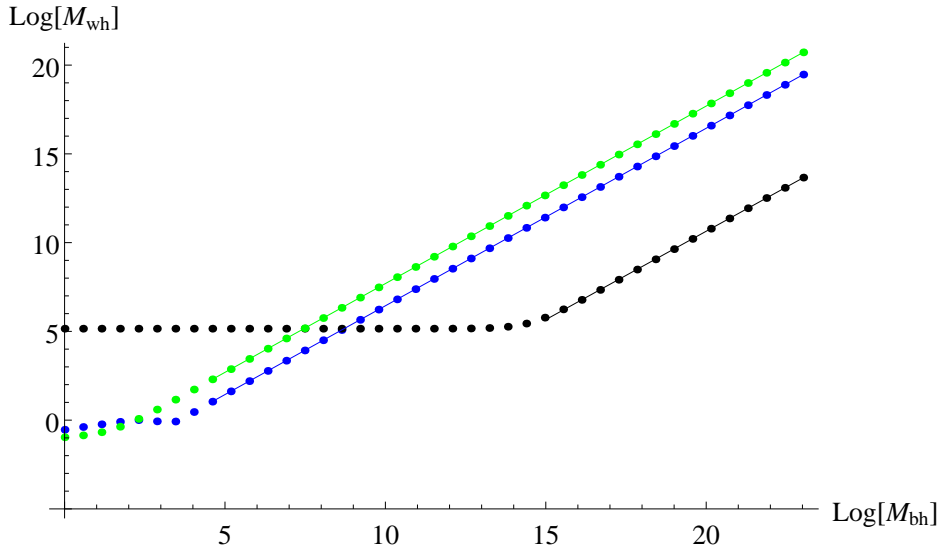


Figure 2. The logarithm of the mass associated to the “white hole” horizon M_{wh} is plotted versus the logarithm of the initial black hole mass M_{bh} , ranging from 1 to 10^{10} in Planck units. The black, blue and green dots correspond respectively to the masses obtained using the Hamiltonians $H_{\text{eff}}^{(1)}$, $H_{\text{eff}}^{(2)}$ and $H_{\text{eff}}^{(3)}$, with the fits for large masses given as $-9.2765 + 0.9958 \log[M_{\text{bh}}]$, $-3.5594 + 1.0000 \log[M_{\text{bh}}]$ and $-2.3075 + 0.9999 \log[M_{\text{bh}}]$ respectively. We take $G = c = 1$, $\beta = 0.2375$, $\mu_a = 1/2$ and $\mu_b = \pi/4$.

important to stress again that in general the relation between the initial black hole mass and the mass associated to the “white hole” horizon strongly depends on the choice of the initial condition a^0 and of the μ parameters. In particular, the relation $M_{\text{wh}} \propto M_{\text{bh}}$ is a consequence of the choice (10) for a^0 , and that the μ parameters are fixed numbers independent of the phase space⁶. But for instance, if one takes μ_b to be dependent of the black hole initial mass as $\mu_b \propto M_{\text{bh}}^{-1}$, while keeping μ_a and a^0 as above, then in the case of the Hamiltonian $H_{\text{eff}}^{(1)}$ one asymptotically obtains that $M_{\text{wh}} \propto M_{\text{bh}}^4$. If one additionally takes a^0 to be a phase space constant (i.e., independent of M_{bh}) we obtain $M_{\text{wh}}^{(1)} \propto M_{\text{bh}}^5$.

V. SUMMARY & DISCUSSION

In this paper we presented the construction of two new effective Hamiltonians for Kantowski-Sachs: $H_{\text{eff}}^{(2)}$ is obtained following the prescription introduced in [35], namely, regularizing the Euclidean part via (11) and then using Thiemann identities for the Lorentzian part; $H_{\text{eff}}^{(3)}$ is derived from the expectation value of Thiemann LQG Hamiltonian on a semiclassical state peaked on Kantowski-Sachs spacetime. We then compared the dynamics in the μ_o -scheme generated by these effective Hamiltonians – as well as the

⁶ Different values of the μ parameters do not alter neither the qualitative properties of the evolution, nor the relation between the initial black hole mass and the mass associated to the “white hole” horizon.

one generated by the effective Hamiltonian $H_{\text{eff}}^{(1)}$ introduced in [21] – with initial conditions at the black hole horizon ($T = T_0 = 0$). The analysis reveals that the integral curves of $H_{\text{eff}}^{(2)}$ and $H_{\text{eff}}^{(3)}$ are similar, but not identical. On the other hand, they are qualitatively different from the ones of $H_{\text{eff}}^{(1)}$. However, in all these cases the singularity is replaced with a black hole to “white hole” transition, and the relations between the initial black hole mass and the final “white hole” mass have asymptotically ($M_{\text{bh}} \gg 1$) the same dependence. Note that the similarity between $H_{\text{eff}}^{(2)}$ and $H_{\text{eff}}^{(3)}$ may suggest that the discrepancy between their dynamics is due to the fact that $H_{\text{eff}}^{(3)}$ is an expansion to finite order in μ , while $H_{\text{eff}}^{(2)}$ is exact; but comparison of the dynamics of the expansion of $H_{\text{eff}}^{(2)}$ with the dynamics of $H_{\text{eff}}^{(3)}$, shows that they are different already at the next-to-leading order. We must therefore conclude that they are indeed two different effective Hamiltonians, but which generate similar dynamics in the μ_o -scheme for the initial conditions we considered.

As mentioned earlier, our analysis is realized in the μ_o -scheme. This scheme is known to produce unphysical results in cosmology (such as a bounce at an energy density much lower than the Planck scale). However, μ_o -scheme models are useful in order to extract the qualitative behavior of such effective models and grasp an understanding of the modifications with respect to the classical theory. One can of course develop the models in the $\bar{\mu}$ -scheme using the Hamiltonians we considered above. In fact, recent proposals [23, 24] study models with the effective Hamiltonian $H_{\text{eff}}^{(1)}$ but with μ ’s being phase space functions. The authors then reach different conclusions about the relations between the initial black hole mass and the final “white hole” mass. Implementing the $\bar{\mu}$ -scheme with the Hamiltonians $H_{\text{eff}}^{(2)}$ and $H_{\text{eff}}^{(3)}$ will require more elaborate analysis, and it is currently under investigation.

Finally, let us mention that our study was limited to spherically symmetric and static spacetime, namely Schwarzschild black hole interior. Further studies following a similar construction could be carried out in the context of non-static solutions, in which case one has to include the exterior of a black hole where the radial dependence cannot be ignored. While this is technically more involved, if successful, it would give us access to modeling physically realistic black holes, describing for example a spherical collapse. It might also give us a way to quantify the transition time involved in the black hole \rightarrow “white hole” process, which would allow to make falsifiable predictions.

ACKNOWLEDGMENTS

The authors would like to thank Jerzy Lewandowski for illuminating discussions. M. A. acknowledges the support of the project BA 4966/1-1 of the German Research Foundation (DFG) and the support of the Polish Narodowe Centrum Nauki (NCN) grant 2011/02/A/ST2/00300. K. L. thanks the German National Merit Foundation and NSF grant PHY-1454832 for their financial support.

- [1] C. Rovelli, *Quantum Gravity*, Cambridge University Press (2004)
- [2] A. Ashtekar and J. Lewandowski, Background independent quantum gravity: A Status report, *Class. Quant. Grav.* **21** R53 (2004)
- [3] T. Thiemann, *Modern Canonical Quantum General Relativity*, Cambridge University Press (2007)
- [4] M. Bojowald, Loop Quantum Cosmology, *Living Rev. Relativity* **8** 11 (2005)
- [5] A. Ashtekar, Loop Quantum Cosmology: An Overview, *Gen. Rel. Grav.* **41** 707-741 (2009)
- [6] A. Ashtekar and P. Singh, Loop Quantum Cosmology: A Status Report, *Class. Quant. Grav.* **28** 213001 (2011)
- [7] A. Ashtekar, T. Pawłowski and P. Singh, Quantum Nature of the Big Bang, *Phys. Rev. Lett.* **96** 141301 (2006)
- [8] A. Ashtekar, T. Pawłowski and P. Singh, Quantum Nature of the Big Bang: An Analytical and Numerical Investigation, *Phys. Rev. D* **73** 124038 (2006)

- [9] A. Ashtekar, T. Pawłowski and P. Singh, Quantum Nature of the Big Bang: Improved dynamics, *Phys. Rev. D* **74** 084003 (2006)
- [10] R. Kantowski, R. Sachs, Some spatially inhomogeneous dust models, *J. Math. Phys.* **7** (3) (1966)
- [11] T. Thiemann, H. Kastrup, Canonical Quantization of Spherically Symmetric Gravity in Ashtekar's Self-Dual Representation, *Nucl. Phys. B* **399** 211-258 (1993)
- [12] T. Thiemann, H. Kastrup, Spherically Symmetric Gravity as a Completely Integrable System, *Nucl. Phys. B* **425** 665-686 (1994)
- [13] M. Bojowald, Spherically symmetric quantum geometry: States and basic operators, *Class. Quant. Grav.* **21**, 3733 (2004)
- [14] V. Husain and O. Winkler, Quantum resolution of black hole singularities, *Class. Quant. Grav.* **22**, L127 (2005)
- [15] M. Bojowald and R. Swiderski, Spherically symmetric quantum geometry: Hamiltonian constraint, *Class. Quant. Grav.* **23**, 2129 (2006)
- [16] R. Gambini and J. Pullin, Black holes in loop quantum gravity: The Complete space-time, *Phys. Rev. Lett.* **101** 161301 (2008)
- [17] A. Ashtekar and M. Bojowald, Quantum Geometry and the Schwarzschild singularity, *Class. Quant. Grav.* **23** 391-411 (2006)
- [18] L. Modesto, Loop quantum black hole, *Class. Quant. Grav.* **23** 5587-5602 (2006)
- [19] C. G. Boehmer and K. Vandersloot, Loop quantum dynamics of Schwarzschild interior, *Phys. Rev. D* **76** 1004030 (2007)
- [20] D. W. Chiou, Phenomenological loop quantum geometry of the Schwarzschild black hole, *Phys. Rev. D* **78** 064040 (2008)
- [21] A. Corichi and P. Singh, Loop quantum dynamics of Schwarzschild interior revisited, *Class. Quant. Grav.* **33** 055006 (2016)
- [22] J. Olmedo, S. Saini and P. Singh, From black holes to white holes: a quantum gravitational symmetric bounce, *Class. Quant. Grav.* **34** 225011 (2017)
- [23] A. Ashtekar, J. Olmedo and P. Singh, Quantum extension of the Kruskal spacetime, *Phys. Rev. D* **98** 126003 (2018)
- [24] N. Bodendorfer, F. M. Mele and J. Mnch, Effective Quantum Extended Spacetime of Polymer Schwarzschild black hole, arXiv:1902.04542 [gr-qc].
- [25] T. Thiemann, Quantum Spin Dynamics (QSD), *Class.Quant.Grav.* **15** 839-873 (1998)
- [26] T. Thiemann, Quantum Spin Dynamics (QSD) II, *Class.Quant.Grav.* **15** 875-905 (1998)
- [27] E. Alesci, M. Assanioussi and J. Lewandowski, Curvature operator for loop quantum gravity, *Phys. Rev. D* **89**, no. 12, 124017 (2014)
- [28] E. Alesci, M. Assanioussi, J. Lewandowski and I. Mkinen, Hamiltonian operator for loop quantum gravity coupled to a scalar field, *Phys. Rev. D* **91**, no. 12, 124067 (2015)
- [29] M. Assanioussi, J. Lewandowski and I. Mkinen, New scalar constraint operator for loop quantum gravity, *Phys. Rev. D* **92**, no. 4, 044042 (2015)
- [30] M. Bojowald, Loop quantum cosmology. 3. Wheeler-Dewitt operators, *Class. Quant. Grav.* **18**, 1055 (2001)
- [31] M. Bojowald, Isotropic loop quantum cosmology, *Class. Quant. Grav.* **19**, 2717 (2002)
- [32] M. Bojowald, Homogeneous loop quantum cosmology, *Class. Quant. Grav.* **20**, 2595 (2003)
- [33] M. Bojowald, G. Date and K. Vandersloot, Homogeneous loop quantum cosmology: The Role of the spin connection, *Class. Quant. Grav.* **21**, 1253 (2004)
- [34] J. Yang, Y. Ding and Y. Ma, Alternative quantization of the Hamiltonian in loop quantum cosmology II: Including the Lorentz term, *Phys. Lett. B* **682** 1-7 (2009)
- [35] M. Assanioussi, A. Dapor, K. Liegener and T. Pawłowski, Emergent de Sitter epoch of the quantum Cosmos, *Phys. Rev. Lett.* **121** 081303 (2018)
- [36] M. Assanioussi, A. Dapor, K. Liegener and T. Pawłowski, Emergent de Sitter epoch of the Loop Quantum Cosmos: a detailed analysis, arXiv:1906.05315 [gr-qc].
- [37] A. Dapor and K. Liegener, Cosmological Effective Hamiltonian from full Loop Quantum Gravity, *Phys. Lett. B* **785** 506-510 (2018)
- [38] A. Ashtekar, New variables for classical and Quantum Gravity, *Phys. Rev. Lett.* **57** (1986)
- [39] A. Ashtekar, Old problems in the light of new variables, *Contemporary Math* **71** (1988)
- [40] J.F. Barbero, Real ashtekar variables for lorentzian signature space times, *Phys. Rev. D* **51** (1995)
- [41] E. Alesci and F. Cianfrani, Quantum-Reduced Loop Gravity: Cosmology, *Phys. Rev. D* **87** 083521 (2013)

- [42] A. Dapor and K. Liegener, Cosmological Coherent State Expectation Values in LQG I. Isotropic Kinematics, *Class. Quant. Grav.* **35** 135011 (2018)
- [43] V. Taveras, Corrections to the Friedmann Equations from LQG for a Universe with a Free Scalar Field, *Phys. Rev. D* **78** 064072 (2008)
- [44] T. Thiemann, Gauge Field Theory Coherent States (GCS): I. General Properties, *Class. Quant. Grav.* **18** 2025-2064 (2001)
- [45] T. Thiemann and O. Winkler, Gauge Field Theory Coherent States (GCS): II. Peakedness Properties, *Class. Quant. Grav.* **18** 2561-2636 (2001)
- [46] T. Thiemann and O. Winkler, Gauge Field Theory Coherent States (GCS): III. Ehrenfest Theorems, *Class. Quant. Grav.* **18** 4629-4682 (2001)
- [47] H. Sahlmann, T. Thiemann and O. Winkler, Coherent States for Canonical Quantum General Relativity and the Infinite Tensor Product Extension. *Nucl. Phys. B* **606** (2001)
- [48] A. Dasgupta, Coherent states for black holes, *JCAP* **08** 004 (2003)
- [49] E. Livine and S. Speziale, A new spinfoam vertex for quantum gravity, *Phys. Rev. D* **76**, 084028 (2007).
- [50] B. Bahr and T. Thiemann, Gauge-invariant coherent states for Loop Quantum Gravity I: Abelian gauge groups. *Class. Quant. Grav.* **26** (2009)
- [51] B. Bahr and T. Thiemann, Gauge-invariant coherent states for Loop Quantum Gravity II: Non-abelian gauge groups. *Class. Quant. Grav.* **26** (2009)
- [52] A. Zipfel and T. Thiemann. Stable coherent States. *Phys rev. D* **93** (2016)
- [53] M. Assanioussi, Polymer quantization of connection theories: Graph coherent states, *Phys. Rev. D* **98**, no. 4, 045016 (2018)
- [54] K. Giesel, T. Thiemann, Algebraic Quantum Gravity (AQG) I. Conceptual Setup, *Class.Quant.Grav.* **24** 2465-2498 (2007)
- [55] K. Giesel, T. Thiemann, Algebraic Quantum Gravity (AQG) II. Semiclassical Analysis, *Class.Quant.Grav.* **24** 2499-2564 (2007)
- [56] T. Thiemann. Quantum Spin Dynamics (QSD): VII Symplectic Structures and Continuum Limit Lattice Formulations of Gauge Field Theories. *Class Quant Grav.* **18** (2001)
- [57] K. Liegener and P. Singh, SU(2) gauge invariant bounce from loop quantum geometry. [arXiv:1906.02759] (2019)
- [58] E. Alesci, S. Bahrami and D. Pranzetti, Quantum evolution of black hole initial data sets: Foundations, *Phys. Rev. D* **98** 046014 (2018)
- [59] E. Alesci, S. Bahrami and D. Pranzetti, Quantum gravity predictions for black hole interior geometry, [arXiv:1904.12412gr-qc] (2019)